

The hyperon mean free paths in the relativistic mean field

Q. L. Wang, L. Dang, X. H. Zhong*, and P. Z. Ning†

Department of Physics, Nankai University, Tianjin 300071, China

The Λ - and Ξ^- -hyperon mean free paths in nuclei are firstly calculated in the relativistic mean field (RMF) theory. The real parts of the optical potential are derived from the RMF approach, while the imaginary parts are obtained from those of nucleons with the relations: $U_S^{IY} = \alpha_{\sigma Y} \cdot U_S^{IN}$ and $U_V^{IY} = \alpha_{\omega Y} \cdot U_V^{IN}$. With the assumption, the depth of the imaginary potential for Ξ^- is $W_{\Xi} \simeq -3.5$ MeV, and for Λ is $W_{\Lambda} \simeq -7$ MeV at low incident energy. We find that, the hyperon mean free path decreases with the increase of the hyperon incident energies, from 200 MeV to 800 MeV; and in the interior of the nuclei, the mean free path is about $2 \sim 3$ fm for Λ , and about $4 \sim 8$ fm for Ξ^- , depending on the hyperon incident energy.

PACS numbers: 21.65.+f, 21.30.Fe

I. INTRODUCTION

The study of the nucleon/hyperon mean free paths in nuclei/nuclear matter is an important aspect for us to know about the nucleon/hyperon in-medium properties, because the nucleon/hyperon mean free paths relate with the nucleon-nucleon/hyperon-nucleon interactions in nuclear matter. In nuclear reactions, the nucleon/hyperon mean free path is a useful concept for summarizing a large number of experimental data, because the nucleon/hyperon mean free path in a nucleus can be introduced from the cross sections of the nucleon/hyperon-nucleus reactions, which can be obtained from experiment directly.

Since the work of Bethe [1] in 1940, there has been considerable interest in the study of the mean free path of a proton or neutron in the nuclear medium [2, 3, 4, 5, 6, 7, 8, 9, 10, 11, 12, 13]. However, theoretical calculation on hyperon mean free path in nuclear medium has never been done due to the scarce experimental data on hyperon-nucleon/nucleus interactions. Recently, some experimental progresses on hyperon increased the necessary for the study of the hyperon mean free path in nuclei. In this paper, we will firstly attempt to calculate the hyperon mean free paths in nuclei in the framework of RMF theory.

The RMF theory have been used to study the nucleon mean free paths [6, 9, 10, 11]. With RMF method, the nucleon mean free path was found to be in reasonable agreement with experimental data. Thus, in present work, we also study the Λ and Ξ^- -hyperon mean free paths in nuclei with RMF method. To calculate the hyperon mean free path in a nucleus, the essential point is to construct the energy-dependent hyperon-nucleus optical potentials. In this work, the real scalar and vector potentials are given by RMF. We attempt to obtain the hyperon imaginary potentials from those of nucleons U_S^{IN} and U_V^{IN} by the relations: $U_S^{IY} = \alpha_{\sigma Y} \cdot U_S^{IN}$ and

$U_V^{IY} = \alpha_{\omega Y} \cdot U_V^{IN}$. In fact, Cooper *et al.* also suggested to obtain the hyperon imaginary potentials from those of nucleons by means of multiplying a factor about ten years ago[14]. The depth of the imaginary potential for Ξ^- - ^{40}Ca , $W_{\Xi} \approx 3.5$ MeV at $T_{\text{lab}}=100$ MeV, is compatible with the prediction of Batty *et al.*[16], $W_{\Xi} \approx 3$ MeV. We find that, in the central of the nuclei, the hyperon mean free path is about $2 \sim 3$ fm for Λ , and about $4 \sim 8$ fm for Ξ^- , depending on the hyperon incident energy. The hyperon mean free path decreases with the increase of the hyperon incident energy.

This paper is organized as follows. In the subsequent section we outline the hyperon-nucleon interactions in RMF. The details of the complex potentials are described in Sec. III. Then the formulas about the hyperon mean free path are deduced in Sec. IV. The results and discussions are given in Sec. V. Finally a brief conclusion is given in Sec. VI.

II. THE HYPERON-NUCLEON INTERACTIONS IN RMF

Within the framework of RMF theory[17, 18], the effective Lagrangian for hyperon and nucleons can be written as[19, 20]

$$\mathcal{L} = \mathcal{L}_N + \mathcal{L}_Y, \quad (1)$$

where \mathcal{L}_N is the standard Lagrangian for nucleons

$$\begin{aligned} \mathcal{L}_N = & \bar{\Psi}_N (i\gamma_\mu \partial^\mu - g_{\omega N} \gamma_\mu \omega^\mu - M_N - g_{\sigma N} \sigma \\ & - \frac{1}{2} g_{\rho N} \gamma_\mu \vec{\tau}^N \cdot \vec{\rho}^\mu - e \gamma_\mu \frac{1 + \tau_3^N}{2} A_\mu) \Psi_N \\ & + \frac{1}{2} (\partial_\mu \sigma \partial^\mu \sigma - m_\sigma^2) - \frac{1}{3} g_2 \sigma^3 - \frac{1}{4} g_3 \sigma^4 \\ & - \frac{1}{4} \Omega_{\mu\nu} \Omega^{\mu\nu} + \frac{1}{2} m_\omega^2 \omega_\mu \omega^\mu - \frac{1}{4} \vec{R}_{\mu\nu} \cdot \vec{R}^{\mu\nu} \\ & + \frac{1}{2} m_\rho^2 \vec{\rho}_\mu \vec{\rho}^\mu - \frac{1}{4} H_{\mu\nu} \cdot H^{\mu\nu}, \end{aligned} \quad (2)$$

with

$$\Omega_{\mu\nu} = \partial_\nu \omega_\mu - \partial_\mu \omega_\nu,$$

*E-mail: zhongxianhui@mail.nankai.edu.cn

†E-mail: ningpz@nankai.edu.cn

TABLE I: The parametrization of the nucleonic sector (NL-SH). The masses are given in (MeV) and the coupling g_2 in (fm^{-1}).

M_N	939.0	$g_{\sigma N}$	10.444
m_σ	526.065	$g_{\omega N}$	12.945
m_ω	783.0	$g_{\rho N}$	4.383
m_ρ	763.0	g_2	-6.9099
		g_3	-15.8337

$$\begin{aligned}\vec{R}_{\mu\nu} &= \partial_\nu \vec{\rho}_\mu - \partial_\mu \vec{\rho}_\nu, \\ H_{\mu\nu} &= \partial_\nu A_\mu - \partial_\mu A_\nu.\end{aligned}\quad (3)$$

It involves nucleons (Ψ_N), scalar σ mesons (σ), vector ω mesons (ω_μ), vector isovector ρ mesons ($\vec{\rho}_\mu$), and the photon (A_μ). The parameter of the nucleonic sector (NL-SH) are adopted from Ref. [21], which describes properties of nuclear matter as well as of finite nuclei reasonably well. The nucleonic parameter set is presented in Table I.

And \mathcal{L}_Y , the Lagrangian for hyperon yields

$$\begin{aligned}\mathcal{L}_Y &= \bar{\Psi}_Y (i\gamma_\mu \partial^\mu - g_{\omega Y} \gamma_\mu \omega^\mu - M_Y - g_{\sigma Y} \sigma \\ &\quad - \frac{1}{2} g_{\rho Y} \gamma_\mu \vec{\tau}_Y \cdot \vec{\rho}^\mu - e\gamma_\mu \frac{1 + \tau_{3,Y}}{2} A_\mu) \Psi_Y.\end{aligned}\quad (4)$$

where Y stands for the hyperon Λ and Ξ^- , and Ψ_Y is the hyperon field. The Pauli matrices for nucleons and hyperons are written as τ_a^B with τ_3^B being the third component.

The (iso)vector coupling constants for hyperon, $g_{\omega Y}$ and $g_{\rho Y}$, are determined from the constituent quark model (SU(6) symmetry), namely:

$$g_{\omega \Lambda} = 2g_{\omega \Xi} = \frac{2}{3}g_{\omega N}, \quad (5)$$

$$g_{\rho \Xi} = g_{\rho N}, \quad g_{\rho \Lambda} = 0. \quad (6)$$

The scalar coupling constant for hyperon, $g_{\sigma Y}$, are determined by fitting to the potential depth of the corresponding hyperon in normal nuclear density with the following relation[20]

$$\begin{aligned}U_Y &= g_{\sigma Y} \sigma^{eq} + g_{\omega Y} \omega^{eq} \\ &= M_N \left(\frac{M_N^*}{M_N} - 1 \right) \cdot \frac{g_{\sigma Y}}{g_{\sigma N}} + \frac{g_{\omega N}^2}{m_\omega^2} \cdot \frac{g_{\omega Y}}{g_{\omega N}} \rho_0,\end{aligned}\quad (7)$$

where U_Y is the hyperon potential depth in normal nuclear density, σ^{eq} and ω^{eq} are the values of σ and ω fields at saturation, and $M_N^*/M_N = 0.597$ and $\rho_0 = 0.146 fm^{-3}$ for the set NL-SH.

It is well known that the potential well depth of Λ hyperon in nuclear matter is about -30 MeV, so we use $U_\Lambda = -30$ MeV to obtain the coupling constant $g_{\sigma \Lambda}$. However, the experimental data on Ξ^- hypernuclei are very few. Dover and Gal[22] analyzed old emulsion data on Ξ^- hypernuclei and concluded a nuclear potential well depth of $U_\Xi = -21$ to -24 MeV. Fukuda et al. [23] fitted

the very-low-energy part of Ξ^- hypernuclear spectrum in the $^{12}C(K^-, K^+)X$ reaction and estimated the value of U_Ξ to be $-16 \sim -20$ MeV. Recently, E885 at the AGS [24] have indicated a potential depth of $U_\Xi = -14$ MeV or less. Note that these Ξ^- potential depth data are estimated based on Woods-Saxon potentials. Here, we choose $U_\Xi = -16$ MeV to fix $g_{\sigma \Xi}$. According to the NL-SH parameter set for nucleons, we easily obtained the coupling constants $g_{\sigma \Lambda} = 6.4694$, $g_{\omega \Lambda} = 8.630$, $g_{\sigma \Xi} = 3.2623$ and $g_{\omega \Xi} = 4.315$.

III. COMPLEX POTENTIALS

For the nucleon/hyperon, within the framework of RMF, its Dirac equation of motion is given by

$$[-i\alpha \cdot \nabla + U_S^B] + \beta(M_B - U_V^B) \Psi_B = E \Psi_B, \quad (8)$$

where U_S^B and U_V^B are the scalar potential and vector potential for the baryons. B stands for the baryons N , Λ , Ξ^- , respectively. For simplicity, we neglect the Coulomb interaction. To describe the absorptive properties of baryons in nuclei, we set U_S^B and U_V^B are the complex numbers in present work. Here both of the complex potentials U_S^B and U_V^B are written as

$$U_S^B = U_S^{RB} + iU_S^{IB}, \quad (9)$$

$$U_V^B = U_V^{RB} + iU_V^{IB}. \quad (10)$$

The real parts of the scalar potential and vector potential for baryons U_S^{RB} , U_V^{RB} are

$$\begin{aligned}U_S^{RB} &= g_{\sigma B} \sigma_0, \\ U_V^{RB} &= g_{\omega B} \omega_0 + g_{\rho B} \tau_{3,B} \rho_{0,3}.\end{aligned}\quad (11)$$

If we neglected the contributions of isospin to the vector potential of the hyperons and nucleons, the real part of the scalar potential and vector potentials U_S^{RY} , U_V^{RY} for hyperons can be related to those of nucleons with

$$U_S^{RY} = \alpha_{\sigma Y} \cdot U_S^{RN} \quad (12)$$

$$U_V^{RY} = \alpha_{\omega Y} \cdot U_V^{RN}, \quad (13)$$

where $\alpha_{\sigma Y} = g_{\sigma Y} / g_{\sigma N}$ and $\alpha_{\omega Y} = g_{\omega Y} / g_{\omega N}$.

From RMF theory, we can obtain the real parts of the complex potentials only. To calculate the hyperon mean free path, we have to know the imaginary part of complex potentials.

Since there is a simple linear relation between the real part of the hyperon scalar (vector) potential U_S^{RY} (U_V^{RY}) and the nucleon scalar (vector) potential U_S^{RN} (U_V^{RN}) (see Eqs.(12) and (13)), the same linear relation should exist in the relation between the hyperon complex potential U_S^Y (U_V^Y) and the nucleon complex potential U_S^N (U_V^N), which are

$$U_S^Y = \alpha_{\sigma Y} \cdot U_S^N, \quad (14)$$

$$U_V^Y = \alpha_{\omega Y} \cdot U_V^N. \quad (15)$$

According to the above suppose, the imaginary potentials of the hyperon-nucleus potentials can be derived from those of nucleons with the following relations:

$$U_S^{IY} = \alpha_{\sigma Y} \cdot U_S^{IN}, \quad (16)$$

$$U_V^{IY} = \alpha_{\omega Y} \cdot U_V^{IN}. \quad (17)$$

The imaginary parts of the nucleon-nucleus potentials U_S^{IN} and U_V^{IN} are extracted from Ref. [15] directly, which determined by fitting a large number of proton elastic scattering data. In fact, to estimate the imaginary parts of the hyperon-nucleus potentials, cooper *et al.* firstly assumed that the hyperon imaginary potentials could be obtained from those of nucleons by means of multiplying a factor about ten years ago[14].

In RMF theory, in terms of the scalar potential U_S^B and the vector potential U_V^B , the momentum of a baryon propagating in the nuclei can be determined from

$$E = \sqrt{(M_B + U_S^B)^2 + k^2} + U_V^B \quad (18)$$

Replaced the complex potentials U_S^B , U_V^B with Eqs.(9, 10), the Eq.(18) can be rewritten as[11]

$$\frac{k^2}{2M_B} + U = E - M_B + \frac{(E - M_B)^2}{2M_B}, \quad (19)$$

where

$$U = V + iW, \quad (20)$$

with

$$V = U_S^{RB} + \frac{E}{M_B} U_V^{RB} + \frac{1}{2M_B} (U_S^{RB2} - U_V^{RB2} + U_V^{IB2} - U_S^{IB2}), \quad (21)$$

$$W = U_S^{IB} + \frac{E}{M_B} U_V^{IB} + \frac{1}{M_B} (U_S^{RB} U_S^{IB} - U_V^{RB} U_V^{IB}). \quad (22)$$

Note that, $U = V + iW$ can be identified as Schrödinger equivalent potential which is the hyperon optical potential in the non-relativistic approach, Eq.(18) is identical to the non-relativistic dispersion relation, except the relativistic correction, $(E - M_B)^2/2M_B$.

It is seen from the Eqs.(21, 22), the Schrödinger equivalent potentials are energy dependent. At zero momentum of the hyperon, compared with the usual optical potential defined in RMF, $U_{opt} = U_S + U_V$, the Schrödinger equivalent potentials have an additional term, which is the third term in Eq.(21) and (22). How much the third term in Eq.(21)/ (22) contributes to the Schrödinger equivalent potentials, which we will discuss latter.

With the imaginary part of hyperon-nucleus potentials given in Eqs(16, 17), we obtain the real part of the hyperon optical potential in Eq. (21)

$$V = U_S^{RY} + \frac{E}{M_Y} U_V^{RY} + \frac{1}{2M_Y} (U_S^{RY2} - U_V^{RY2} + \alpha_{\omega Y}^2 U_V^{IN2} - \alpha_{\sigma Y}^2 U_S^{IN2}), \quad (23)$$

and the imaginary optical potential strength is then obtained in Eq. (22):

$$W = \alpha_{\sigma Y} U_S^{IN} + \alpha_{\omega Y} \frac{E}{M_Y} U_V^{IN} + \frac{1}{M_Y} (\alpha_{\sigma Y} U_S^{RY} U_S^{IN} - \alpha_{\omega Y} U_V^{RY} U_V^{IN}) \quad (24)$$

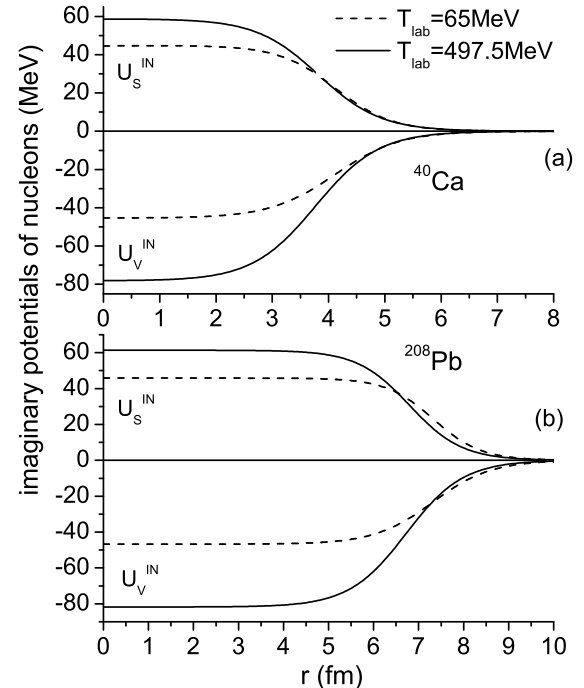


FIG. 1: The imaginary scalar potential, U_S^{IN} and vector potential, U_V^{IN} for N in ^{40}Ca and ^{208}Pb at the $T_{\text{lab}} = 65$ and 497.5 MeV, respectively.

IV. HYPERON MEAN FREE PATH IN RMF

Since the potentials U_S^Y and U_V^Y are complex, the hyperon momentum k is also complex and can be expressed as

$$k = k_R + ik_I. \quad (25)$$

The hyperon mean free path, λ , is related to the imaginary part of the hyperon momentum by

$$\lambda = \frac{1}{2k_I}. \quad (26)$$

From equations (19), (20), (25) and (26), it is easy to derive an analytical expression for λ ,

$$\lambda = \frac{1}{2} \left\{ -M_Y \left(E - M_Y - V + \frac{(E - M_Y)^2}{2M_Y} \right) + M_Y \cdot \left[\left(E - M_Y - V + \frac{(E - M_Y)^2}{2M_Y} \right)^2 + W^2 \right]^{\frac{1}{2}} \right\}^{-\frac{1}{2}} \quad (27)$$

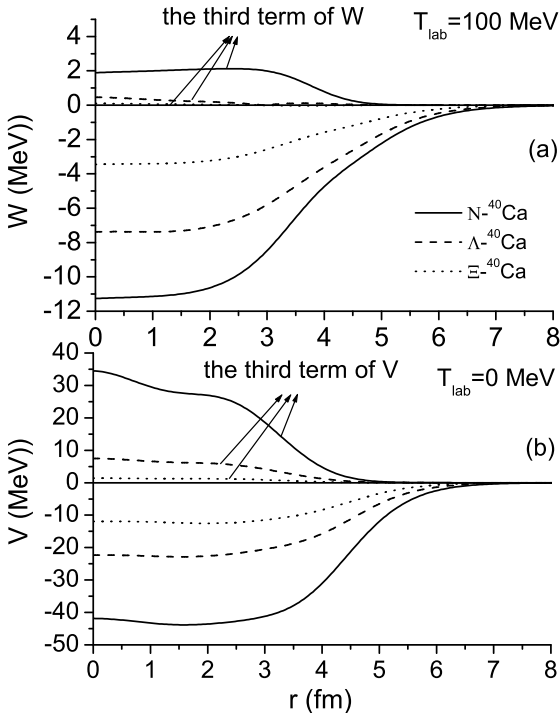


FIG. 2: The Λ - ^{40}Ca , Ξ - ^{40}Ca and N - ^{40}Ca potentials are showed. We showed their real potentials at the $T_{\text{lab}} = 0$ MeV in Fig. (b) and their imaginary parts at the $T_{\text{lab}} = 100$ MeV in Fig. (a).

For a hyperon propagating in a nucleus, its total energy E is related to the incident energy T_{lab} by

$$E = \frac{M_Y^2 + m_T(M_Y + T_{\text{lab}})}{[(M_Y + m_T)^2 + 2m_T T_{\text{lab}}]^{1/2}}, \quad (28)$$

where m_T is the mass of nucleus.

V. RESULTS AND DISCUSSION

In Fig. 1, we plot the imaginary parts of the nucleon-nucleus potentials as functions of radial radii r at incident energy $T_{\text{lab}} = 65$ and 497.5 MeV, respectively. Obviously, the results of U_S^{IN} and U_V^{IN} in Ref. [15] are repeated.

According to Eqs. (23), (24), we can easily obtain the energy dependent Schrödinger equivalent potentials for the Λ and Ξ^- hyperons. As an example, in Fig. 2, the nucleon, Λ , Ξ^- Schrödinger equivalent potentials in ^{40}Ca are shown. To compare with the usual RMF optical potential, we set $T_{\text{lab}} = 0$ and plot the real Schrödinger equivalent potential V in Fig. 2 (b). Because the imaginary nucleon-nucleus potentials are fitted at $T_{\text{lab}} \geq 65$ MeV, we set $T_{\text{lab}} = 100$ MeV and plot the imaginary part W in Fig. (a).

From the figure, we can see that the real parts of the depth of the Schrödinger equivalent potential are -12 ,

-22 and -42 MeV for Ξ^- , Λ and nucleon, respectively. The contributions of the third term in Eqs. (23) to the real part of the Schrödinger equivalent potential are about 7 MeV for Λ - ^{40}Ca and even reaches 35 MeV for N - ^{40}Ca , however the contributions to Ξ^- - ^{40}Ca is no more than 1 MeV. As a whole, the depth of the usual RMF optical potential is deeper than the Schrödinger equivalent potential. For N - ^{40}Ca and Λ - ^{40}Ca , there are large differences between the usual RMF optical potential and the Schrödinger equivalent potential.

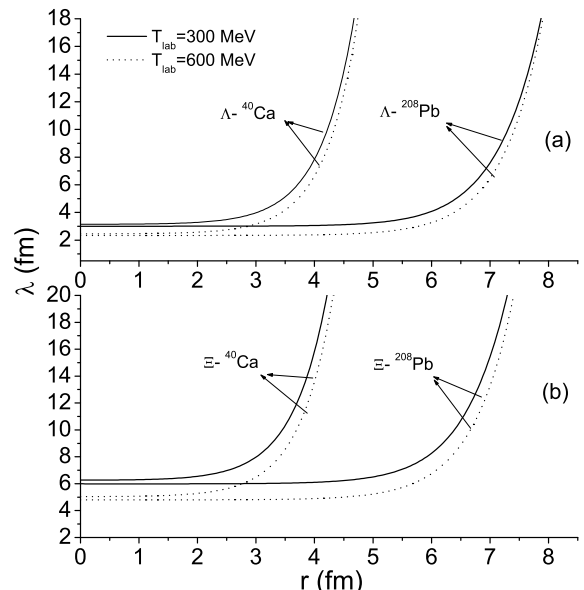


FIG. 3: The hyperon mean free path varied with the radius in ^{40}Ca and ^{208}Pb , with the incident energies, $T_{\text{lab}} = 300$ MeV and 600 MeV. Which for Λ hyperon are showed in Fig. (a) and the Ξ^- hyperon's are shown in Fig. (b).

There are few works about the imaginary optical potentials for the hyperons before. For Ξ^- , Dover and Gal suggested an imaginary part strength of ~ -1 MeV[22]. While Batty *et al.* suggested that the depth of imaginary optical potential for Ξ^- is about 3 MeV, which is calculated with a $t\rho$ potential with $\text{Im}b_0=0.04$ fm [16]. From the figure, we find our prediction for depth of the imaginary optical potential for Ξ^- -Ca at low incident energy ($T_{\text{lab}} = 100$ MeV) is $W_{\Xi} \approx -3.5$ MeV, which is compatible with that of Batty *et al.*. It indicates that our assumption for the imaginary potentials in Eqs.(16) and (17) is reasonable. For Λ , we predicted the depth of the imaginary potential is $W_{\Lambda} \simeq -7$ MeV. The depth of the imaginary potential for nucleon is $W_N \simeq -11$ MeV. In the imaginary optical potential for Ξ , Λ and N , the deepest one is for N , the lowest one is for Ξ^- . The contributions of the last term in Eq. (24) to the imaginary potentials for Ξ , Λ and N is small, which are neglectable for Ξ , Λ .

With the determined potentials, we can calculate the

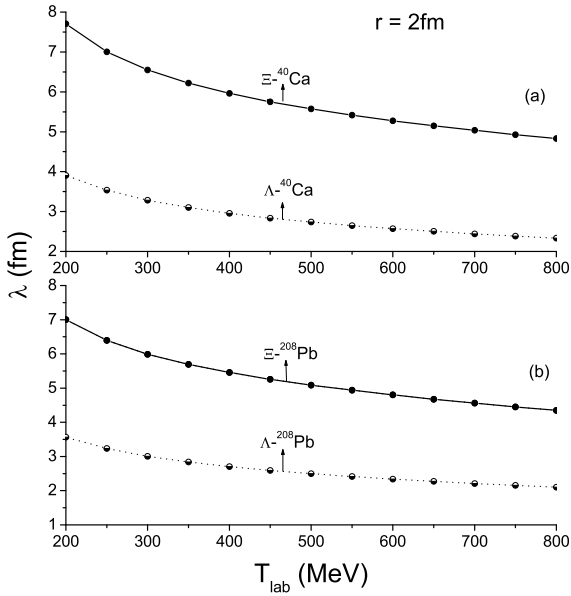


FIG. 4: The Λ , Ξ^- hyperon mean free path varied with the incident energies, T_{lab} , from 200 MeV to 800 MeV in ^{40}Ca and ^{208}Pb at $r = 2$ fm in Fig. (a) and (b) respectively.

hyperon mean free path in nuclei. We show the hyperon Λ , Ξ^- mean free path in ^{40}Ca and ^{208}Pb as function of the radial distance r in Fig. 3. The solid, dotted curves correspond to the hyperon incident energies $T_{\text{lab}} = 300$ MeV and 600 MeV, respectively. In the center of the nuclei, the mean free path is about $2 \sim 3$ fm for Λ , and about $5 \sim 6$ fm for Ξ^- , depending on the the hyperon incident energy. The mean free path is nearly independent of a certain nucleus. The hyperon mean free path increases rapidly at the surface of the nucleus due to the decrease of the hyperon-nucleus interactions.

To see the effects of the hyperon incident energy on the mean free path clearly, we also plot the mean free path in ^{40}Ca and ^{208}Pb (with $r = 2$ fm) as a function of incident energy T_{lab} in Fig. 4. From the figure, we find the hyperon mean free path decreases with the increase of the hyperon incident energy. At $T_{\text{lab}} = 200$ MeV, the free mean path in ^{40}Ca and ^{208}Pb for Λ (Ξ^-) is about 7.8 and 7 (4 and 3.5) fm, respectively, while at $T_{\text{lab}} = 800$ MeV, which decreases to about 5 and 4.5 (2.5 and 2) fm.

VI. CONCLUSION

We have constructed the energy dependent Schrödinger equivalent potentials for hyperon-nucleus,

which are functions of scalar and vector potentials. The real scalar and vector potentials for hyperons are obtained from RMF theory directly. With the assumption, $U_S^Y = \alpha_{\sigma Y} U_S^N$ and $U_V^Y = \alpha_{\omega Y} U_V^N$, we relate the hyperon imaginary potentials with the nucleon's, which are $U_S^{IY} = \alpha_{\sigma Y} U_S^{IN}$ and $U_V^{IY} = \alpha_{\omega Y} U_V^{IN}$. The imaginary scalar and vector potentials, U_S^{IN} and U_V^{IN} , are obtained from Ref. [15], which determined by fitting a large number of proton elastic scattering data. At low incident energy, the depth of the imaginary potential W for hyperon-nucleon is on the order of several MeV. We calculate the depth of the imaginary potential for Ξ^- - ^{40}Ca , $W_{\Xi} \approx 3.5$ MeV at $T_{\text{lab}}=100$ MeV, which is compatible with the prediction of Batty *et al.*[16], $W_{\Xi} \approx 3$ MeV. The imaginary potential is $W_{\Lambda} \simeq -7$ MeV for Λ - ^{40}Ca .

With the determined potentials, we calculated the Λ , Ξ^- -hyperon mean free path in ^{40}Ca , ^{208}Pb with incident hyperon kinetic energy from 200 MeV to 800 MeV. In the interior of the nuclei, the hyperon mean free path less depends on a certain nucleus, and the mean free path is about $2 \sim 3$ fm for Λ , and about $4 \sim 8$ fm for Ξ^- , depending on the hyperon incident energy. The hyperon mean free path decreases with the increase of the hyperon incident energy.

Because there were few works about the hyperon mean free path and hyperon-nucleus imaginary potential before, the present work is only an attempt in this field. Many theoretical as well as experimental works are waiting to be done. Besides, the study of the temperature dependence of the hyperon mean free path are also needed due to the appearance of hyperons in high-energy heavy-ion reactions.

Acknowledgements

This work was supported by the Natural Science Foundation of China (10275037, 10575054), the Doctoral Programme Foundation of the China Institution of Higher Education (20010055012) and the Science and Technology Innovation Foundation of Nankai University, China. The authors would like to thank Chunyan Song for the useful discussion, and thank Haixia An for our code.

- [3] M. T. Collins and J. J. Griffin, Nucl. Phys. **A348**, 63 (1980).
- [4] J. W. Negele and K. Yazaki, Phys. Rev. Lett. **47**, 71 (1981).
- [5] C. Mahaux, Phys. Rev. C **28**, 1848 (1983).
- [6] T. Cheon, Phys. Rev. C **38**, 1516 (1988).
- [7] H. J. Yuan, H. L. Lin, G. Fai and S. A. Moszkowski, Phys. Rev. C **40**, 1448 (1989).
- [8] G. Q. Li, J. of Phys. G **17**, 1 (1991).
- [9] R. A. Rego, Phys. Rev. C **44**, 1944 (1991).
- [10] B. C. Clark et al., Phys. Lett. B **229**, 189 (1993).
- [11] G. Q. Li, R. Machleidt, and Y. Z. Zhuo, Phys. Rev. C **48**, 1063 (1993).
- [12] J. C. Caillou and J. Labarsouque, Phys. Rev. C **54**, 2069 (1996).
- [13] Lie-Wen Chen, Feng-Shou Zhang, Zhao-Hui Lu, and Hong-Ru Ma, Phys. Rev. C **64**, 064315 (2001).
- [14] E. D. Cooper, B. K. Jennings, and J. Mareš, Nucl. Phys. A **580**, 419 (1994); A **585**, 157c (1995).
- [15] S. Mama et al., Phys. Rev. C **41**, 2737 (1990).
- [16] C.J. Batty, E. Friedman, and A. Gal, Phys. Rev. C **59**, 295 (1999).
- [17] B. D. Serot and J. D. Walecka, Adv. Nucl. Phys. **16**, 1 (1986).
- [18] P.-G. Reinhard, Rep. Prog. Phys. **52**, 439 (1989).
- [19] Y. H. Tan, Y. A. Luo, P. Z. Ning, and Z. Y. Ma, Chin. Phys. Lett. **18**, 1030 (2001).
- [20] Y. H. Tan, X. H. Zhong, C. H. Cai, and P. Z. Ning, Phys. Rev. C **70**, 054306 (2004).
- [21] M. M. Sharma, M. A. Nagarajan, and P. Ring, Phys. Lett. B **312**, 377 (1993).
- [22] C. B. Dover and A. Gal, Ann. Phys. (N.Y.) **146**, 309 (1983).
- [23] T. Fukuda et al., Phys. Rev. C **58**, 1306 (1998).
- [24] P. Khaustov et al., Phys. Rev. C **61**, 054603 (2000).